L. HORNÝ, H. CHLUP, R. ŽITNÝ,
T. ADÁMEK

CONSTITUTIVE MODELING OF CORONARY ARTERY BYPASS GRAFT WITH INCORPORATED TORSION

The aim of this study is to describe mechanical response of coronary artery bypass graft (CABG). Attention was paid to sensitivity of a model to small torsions superimposed to an inflation and extension of an artery. The inflation-extension test was performed. A presence of torsions was proved via displacements analysis based on digital image correlation. CABG was modeled as nonlinearly hyperelastic, anisotropic and incompressible material with thin-walled cylindrical geometry. A strain energy function based on limiting fiber extensibility was used. Estimation of material parameters led to good agreement between the model and observations. It was concluded that the model is insensitive to small torsions superimposed to inflation-extension of the artery.

Key words: *Coronary artery bypass graft, constitutive model, digital image correlation, limiting fiber extensibility, saphenous vein*

INTRODUCTION

Coronary artery bypass graft (CABG) is still frequent revascularization technique especially for advanced coronary artery disease. Biomechanical research of CABG is mainly aimed to investigation of hemodynamical conditions, which are believed to play the most important role in CABG failure, e.g. [1], [2]. An implantation of venous CABG into an arterial system starts remodeling and adaptation processes that may lead to new stenosis or luminal narrowing. Implanted venous tissue adapts itself not only due to changed wall shear stress but also due to change in magnitude of pressure pulsations [3], [4]. Adaptation processes may lead to intimal hyperplasia and consecutive thickening of an artery. An anastomotic technique may also significantly affect stress state and hemodynamics of a graft [5], [6].

Experimental research in biomedical engineering should afford reliable results in constitutive modeling of CABG tissue in order to elucidate above mentioned phenomenon. Nevertheless, such papers concerning constitutive modeling of CABG are rare. Hence, main goal of this study is to present constitutive behaviour of the CABG.

Experimental methods, an inflation-extension test, and data post processing, are described first. Special attention is paid to *digital image correlation* (DIC), which was used in order to evaluate kinematical quantities. In contrast to authors' previous report dealing with CABG [7], here main attention is paid to assessment of a twist which accompanied an inflation and extension of a sample within experimental procedure. The paper continues with description of a constitutive model based on *limiting fibre extensibility*. Finally, the estimation of material parameters based on membranous stresses in a thin-walled tube is presented.

EXPERIMENT

The CABG tissue was harvested within autopsy at the Institute of Forensic Medicine of the Faculty Hospital Kralovske Vinohrady in Prague from 66–year–old male donor who did not die in the link with cardiovascular diseases. After autopsy the sample was stored in the saline solution at temperature 4°C. The inflation-extension test was finished 65 hours after death. All measurements were performed under room temperature. Experiments were performed 35 months after the bypass surgery. Grafting material used in the bypass surgery was gained from a saphenous vein.

The reference configuration of the CABG sample had approximately a tubular shape with the following referential dimensions: outer radius R_o = 2.31 mm; thickness H = 0.25 mm. Residual strains, that cause opening

─────────
L.Horny, H.Chlup, R.Zitny, Faculty of Mechanical Engineering Czech Technical University in Prague, Prague, Czech Republic, T.Adamek, Third Faculty of Medicine, Charles University in Prague, Prague, Czech Republic, H.Chlup, Institute of Thermomechanics, Czech Academy of |Science, Prague, Czech Republic

of an arterial ring after radial cut, were immeasurable by our standard equipment (compliance of the sample did not allowed appropriate manipulations). Thus in the following no residual stresses are presumed. The sample was dusted over by pepper and coffee powder to create an artificial surface layer with a stochastic pattern and mounted into the experimental set up for the inflation–extension test.

The experimental configuration was vertical and the tube had closed end. The sample is shown in the Fig. 1. The tube was pressurized manually by a syringe. After preconditioning period (approx. 2 minutes pressurization) measurement cycles were performed. Internal pressure was measured by a pressure probe (KTS 438, Cressto, Czech Rep.) and recorded into PC. Kinematics of the inflation and extension was recorded by digital cameras that are components of DIC system Q–450 (DANTEC Dynamics, Germany).

Figure 1. **The sample of CABG mounted into the experimental set-up**

The measurement cycles were recorded for 1 minute. The pressure ranged from 0 up to 20 kPa. Four recorded cycles span to 60 seconds. Experimental procedure was repeated with different values of suspended weight as described in [7]. In present paper, the attention is focused only on cycles performed with no weight.

DATA POST-PROCESSING

Kinematics of the experiment was recorded and evaluated by digital image correlation (DIC). The DIC is an optical method for 3D non-contact measurement of displacements and deformations based on an analysis of grey value digital images. Principles of displacements and strain evaluation by DIC are presented in [8,9,10].

Briefly, DIC is based on stereoscopic view when each material point is focused on a specific pixel in the image plane of the respective sensor. If the imaging parameter for each sensor and the orientation of the sensors with respect to each other are known, the position of each material point in three dimensions can be calculated. Using a stochastic pattern on the object surface, the position of each material point in two images can be identified by means of correlation algorithm. Such a way particular part of the sample may be monitored. It means that only deformations in the middle part of inflated CABG were incorporated. Successful application of DIC has already been reported in [9]. Recent paper [10] proved successful using DIC for an inflation test in combination with microscope system.

Observed data are summarized in Fig. 2. Presented values of stretches were calculated using (1) and values determined by DIC.

$$\lambda_t = \frac{r_m}{R_m} \qquad \lambda_z = \frac{l}{L} \tag{1}$$

$$l\left(r_o^2 - r_i^2\right) = L\left(R_o^2 - R_i^2\right) \tag{2}$$

Here λ_t and λ_z denote circumferential stretch and axial stretch, respectively. Lower case letters correspond to spatial configuration and capital letters to the geometry under reference configuration. R_m and r_m stand for middle radius in appropriate configuration. Lengths are denoted using l and L. Middle radius is obtained as $(r_i+r_o)/2$, where indices i and o refer to internal and external radius. It should be noted that r_o is observed quantity and r_i is calculated from incompressibility condition (2). Twist angle, ω, was determined from mutual rotations of two contour curves in the middle part of the sample and related to reference length. While upper end of the tube was fixed, it was enabled to extend axially and rotate on its lower end.
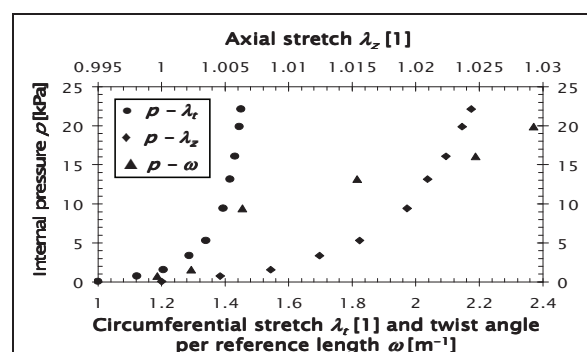

Figure 2. **Mechanical response of the CABG (loading part of selected cycle) COMPUTATIONAL MODEL**

The sample of CABG was assumed to be nonlinearly hyperelastic, anisotropic and incompressible one-layered,

cylindrical thin-walled tube within the entire test. In the present study the material of CABG is modeled as fiber reinforce composite with two families of fibers arranged in symmetrical helices. Both families of fibers are presumed to be mechanically equivalent thus; they are described with the same material parameters. These fibers represent collagenous component of arterial wall, [10,11]. The matrix of the composite is supposed to be isotropic.

Two stored energy functions (SEF) are used in this study. Crucial assumption engaged in anisotropic part of SEF is so-called *limiting fiber extensibility* originally proposed in [13]. This is direct generalization of limiting chain extensibility, which is successfully used in polymer mechanics [14,15]. It means that there exists finite value of fiber stretch (chain stretch) when stored energy tends toward infinity. This property ensures gradual stiffening observed when blood vessels undergo large strains. It is self-evident that real material approaches a failure before this limiting value of a stretch. Anisotropic part of SEF, W, was employed in the form (3).

$$W_{aniso} = \mu_f J_f \, \mathbf{ln}\left(\left(1 - \frac{(I_4-1)^2}{J_f^2}\right)\left(1 - \frac{(I_6-1)^2}{J_f^2}\right)\right)^{-\frac{1}{2}} \quad (3)$$

Here μ_f denotes shear modulus of fibers (stress-like) and J_f is so-called limiting extensibility parameter of fibers. I_4 and I_6 denote additional invariants of right Cauchy-Green strain tensor $\mathbf{C}$ originating from anisotropy, see [11,13]. Particular form of I_4 and I_6 will be described in the following. This anisotropic expression was combined with two equations for isotropic response. First considered was classical neo-Hook model (4).

$$W_{iso}^1 = \frac{\mu_m}{2}\left(I_1 - 3\right) \quad (4)$$

$$W_{iso}^2 = -\frac{\mu_m J_m}{2} \ln\left(1 - \frac{I_1 - 3}{J_m}\right) \quad (5)$$

As second model, it was suggested to use isotropic counterpart of (3) proposed by Gent [14]. This choice might be physically more appropriate because limiting extensibility may be expected in other components of arterial wall. Furthermore, it is well known that suitability of (4) is limited. In equations (4) and (5) μ_m denotes reference shear modulus of the matrix and J_m is limiting extensibility parameter. First invariant of $\mathbf{C}$ is denoted I_1.

Deformation gradient $\mathbf{F}$ maps material points from reference to spatial configuration and on its basis strain tensor $\mathbf{C}$ is defined as $\mathbf{C} = \mathbf{F}^T\mathbf{F}$. The loading of the artery by internal pressure is followed by its inflation, extension and torsion, nevertheless the geometry of the sample is supposed to be maintained cylindrical. Let R, Θ, Z be polar cylindrical coordinates of a material point in the reference configuration and r, θ, z are their counterparts in spatial configuration. Then above-mentioned deformation may be expressed as following mapping (6).

$$r = r(R) \quad \theta = \Theta + \omega Z \quad z = \lambda_z Z \quad (6)$$

Explicit form for r is gained using incompressibility condition (2). Axial stretch, λ_z, is supposed to be constant in the tube. In such a case, deformation gradient has nonzero components as in (7) with tensorial form given in (8).

$$\lambda_R = \frac{1}{\lambda_\Theta \lambda_Z} \quad \lambda_\Theta = \frac{r}{R} \quad \lambda_Z = \frac{l}{L} \quad \gamma = \omega r \lambda_Z \quad (7)$$

Incompressibility condition, $\lambda_R \lambda_\Theta \lambda_Z = 1$, was used in (7a).

$$\mathbf{F} = \lambda_R \boldsymbol{e}_r \otimes \boldsymbol{e}_R + \lambda_\Theta \boldsymbol{e}_\theta \otimes \boldsymbol{e}_\Theta$$
$$\lambda_Z \boldsymbol{e}_z \otimes \boldsymbol{e}_Z + \gamma \boldsymbol{e}_\theta \otimes \boldsymbol{e}_Z \quad (8)$$

Here unit basis vectors are denoted $\boldsymbol{e}_\alpha$. The form of α corresponds to polar cylindrical coordinates in reference or spatial configuration. Detailed analysis of such a situation can be found in [11,16].

If unit vectors aligned with helical reinforcing fibers under reference configuration are expressed as $\boldsymbol{M} = (0,\cos(\beta),\sin(\beta))^T$ and $\boldsymbol{N} = (0,\cos(-\beta),\sin(-\beta))^T$, then additional invariants of $\mathbf{C}$, I_4 and I_6, will be obtained. They are defined as $I_4 = \boldsymbol{M}\cdot(\mathbf{C}\boldsymbol{M})$, $I_6 = \boldsymbol{N}\cdot(\mathbf{C}\boldsymbol{N})$ and after some algebra equations (9) and (10) may be written.

$$I_4 = \lambda_\Theta^2 \cos^2\beta + \lambda_\Theta \gamma \sin 2\beta + \left(\lambda_Z^2 + \gamma^2\right)\sin^2\beta$$

$$I_6 = \lambda_\Theta^2 \cos^2\beta - \lambda_\Theta \gamma \sin 2\beta + \left(\lambda_Z^2 + \gamma^2\right)\sin^2\beta$$

New material parameter, helix angle β, has been appeared in (9,10). Remaining question is the form of I_1. It may be written in the form of (11).

$$I_1 = \lambda_R^2 + \lambda_\Theta^2 + \lambda_Z^2 + \gamma^2 \quad (11)$$

Constitutive equations for incompressible hyperelastic material are given in (12).

$$\boldsymbol{\sigma} = \mathbf{F}\frac{\partial W}{\partial \mathbf{E}}\mathbf{F}^T - p\,\mathbf{I} \quad (12)$$

In tensorial equation (11) $\boldsymbol{\sigma}$, p and $\mathbf{I}$ denote Cauchy stress tensor, Lagrangean multiplier arisen form incompressibility constraint and unit second-order tensor, respectively. Thin-walled assumption allows p to be determined from $\sigma_{rr} = 0$.

Green strain tensor, **E**, is defined in usual manner **E** = ½(**C-I**). Explicit tensorial form is written in (13) and reveals contribution of torsion to axial strain what is substantial.

$$\mathbf{E} = \tfrac{1}{2}\left(\lambda_R^2 - 1\right)\boldsymbol{e}_R \otimes \boldsymbol{e}_R + \tfrac{1}{2}\left(\lambda_\Theta^2 - 1\right)\boldsymbol{e}_\Theta \otimes \boldsymbol{e}_\Theta$$
$$+ \tfrac{1}{2}\left(\lambda_Z^2 + \gamma^2 - 1\right)\boldsymbol{e}_Z \otimes \boldsymbol{e}_Z + \tfrac{1}{2}\lambda_\Theta \gamma \boldsymbol{e}_\Theta \otimes \boldsymbol{e}_Z \quad (13)$$
$$+ \tfrac{1}{2}\lambda_\Theta \gamma \boldsymbol{e}_Z \otimes \boldsymbol{e}_\Theta$$

Constitutive equation (12) gives nonzero components of stress tensor as described in (14-16).

$$\sigma_{\theta\theta} = \lambda_\Theta^2 W_{\Theta\Theta} + 2\lambda_\Theta \gamma W_{\Theta Z} + \gamma^2 W_{ZZ} - p \quad (14)$$

$$\sigma_{zz} = \lambda_Z^2 W_{ZZ} - p \quad (15)$$

$$\sigma_{\theta z} = \lambda_Z \left(\lambda_\Theta W_{\Theta Z} + \gamma W_{ZZ}\right) \quad (16)$$

Where denotation $W_{IJ} = \partial W / \partial E_{IJ}$ was used.

RESULTS

Membranous components of $\boldsymbol{\sigma}$ for thin-walled tube may be determined form external loading and used to fit material parameters. Such an approach is suitable for $\sigma_{\theta\theta}$ and σ_{zz}, where $\sigma_{\theta\theta} = pr_i/(r_o-r_i)$ and $\sigma_{zz} = \tfrac{1}{2}\sigma_{\theta\theta}$ have to be satisfied. However, equation for $\sigma_{\theta z}$ may not be set up on this basis because no torsional couple was measured experimentally.

Least square optimization based on comparison of model predictions (14), (15) and stresses determined form external loading was performed in Maple software using Optimisation package. Material parameters were estimated for two SEF, W^1 and W^2.

$$W^1 = W_{iso}^1 + W_{aniso} \qquad W^2 = W_{iso}^2 + W_{aniso} \quad (17)$$

Estimated material parameters are presented in Tab. 1. Fig. 3 shows comparison between observed data and model predictions. Results for axial force gave correlation coefficients none the worse than 0.99 in every model.

Table 1. **Material parameters**

Model	μ_f [kPa]	J_f [1]	β [°]	μ_m [kPa]	J_m [1]
W^1 torsion	23.15	0.666	44.4	0.5	-
W^1 no torsion	22.65	0.662	44.3	0.5	-
W^2 torsion	23.14	0.666	44.4	0.5	0.723
W^2 no torsion	22.64	0.662	44.4	0.5	0.729

CONCLUSION

Based on observed data it was concluded that the inflation and extension of CABG was accompanied with small torsions. Which was observed despite no couple was applied in lower boundary of the tube. These torsions may originate from non-homogeneity and non-uniformity of the sample, pre-strain in fixed boundary may be of concern too. Two different models of SEF were used to fit material parameters. Both models fit observed data successfully on the level of membranous computational model. Limiting fiber extensibility assumption for anisotropic
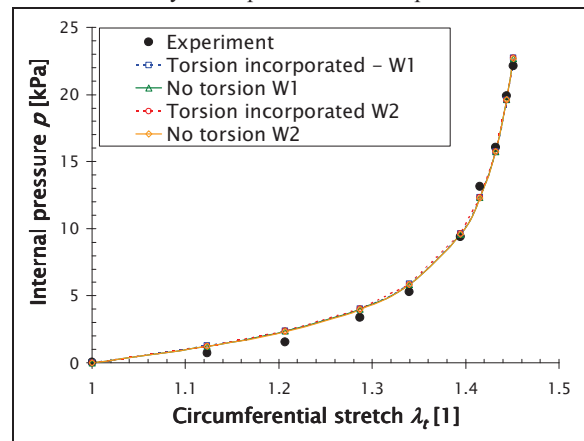

Figure 3. **The fit of observed data**

component of a blood vessel wall and limiting chain extensibility for isotropic component were proven useful. Explicit forms of (9) and (10) revealed that despite of symmetrical arrangement of reinforcement fibers corresponding invariants differ when torsion is considered. The effect of small torsions superimposed to inflation and extension was proven negligible in membrane model. Estimated values of parameters (and model predictions) were similar in both cases, with incorporated torsion and with no torsion.

REFERENCES

[1] L.R. Leask, M.J. Butany, K.W. Johnston, C.R. Ethier, M. Ojha, Annals of Biomedical Engineering, 33 (2005) 3, 301–309.

[2] R. Tran-Son-Tay, M. Hwang, M Garbey, Z. Jiang, C.K. Ozaki, S.A. Berceli, Annals of Biomedical Engineering, 36 (2008) 7, 1083–1091.

[3] C.M. Fernandez, D.R. Goldman, Z. Jiang, C.K. Ozaki, R. Tran-Son-Tay, S.A. Berceli, Annals of Biomedical Engineering, 32 (2004) 11, 1484–1493.

[4] G.S. Kassab, J.A. Navia, Annual Review of Biomedical Engineering, 8 (2006), 499–535.

[5] T. Frauenfelder, E. Boutsianis, T. Schertler, L. Husmann, S. Leschka, D. Poulikakos, B. Marincek, H. Alkadhi, BioMedical Engineering OnLine, **6** (2007) 35. DOI 10.1186/1475-925X-6-35.

[6] F. Cacho, M. Doblaré, G.A. Holzapfel, Medical and Biological Engineering and Computing, 45 (2007) 9, 819–827.

[7] L. Horny, H. Chlup, R. Zitny, T. Adamek, Constitutive behavior of coronary artery bypass graft, in Proceedings of the World Congress on Medical Physics and Biomedical Engineering, 11th International Congress of the IUPESM, 7th – 12th September 2009, Munich, Germany (accepted for publication).

[8] C. Herbst, K. Splitthof, Q–400 Basics of 3D digital image correlation, Dantec Dynamics manual, available on http://www.dantecdynamics.com/Default.aspx?ID=855

[9] D. Zhang, C.D. Eggleton, D.D. Arola, Experimental Mehcanics, 42 (2002) 4, 409–416.

[10] M.A. Sutton, X. Ke, S.M. Lessner, M. Goldbach, M. Yost, F. Zhao, H.W. Schreier, Journal of Biomedical Materielas Research Part A, 84 (2008) 1, 178–190.

[11] G.A. Holzapfel, T.C. Gasser, R.W. Ogden, Journal of Elasticity, 61 (2000) 1-3, 1–48.

[12] T.C. Gasser, R.W. Ogden, G.A. Holzapfel, Journal of the Royal Society Interface, 3 (2006) 6, 15–35.

[13] C.O. Horgan, G. Saccomandi, Journal of the Mechanics and Physics of Solids, 53 (2005) 9, 1985–2015.

[14] A.N. Gent, Rubber Chemistry and Technology, 69 (1996) 1,59–61.

[15] .O. Horgan, G. Saccomandi, Biomechanics and modeling in mechanobiology, 1 (2003) 4, 251–266.

[16] L.A. Taber, Nonlinear Theory of Elasticity Applications in Biomechanics, World Scientific, New Jersey, 2004, pp. 280–294.